

Tryptophan Silver Nanoparticles Synthesized by Photoreduction Method: Characterization and Determination of Bactericidal and Anti-Biofilm Activities on Resistant and Susceptible Bacteria

International Journal of Tryptophan Research
Volume 12: 1–8
© The Author(s) 2019
Article reuse guidelines:
sagepub.com/journals-permissions
DOI: 10.1177/1178646919831677



Daniella dos Santos Courrol¹, Carla Regina Borges Lopes² ,
Camila Bueno Pacheco Pereira¹ , Marcia Regina Franzolin¹ ,
Flávia Rodrigues de Oliveira Silva³ and Lilia Coronato Courrol²

¹Laboratório de Bacteriologia, Instituto Butantan, São Paulo, Brazil. ²Laboratório de Lasers e Óptica Biomédica Aplicada and Departamento de Física, Universidade Federal de São Paulo, Diadema, Brazil. ³Centro de Ciência e Tecnologia de Materiais, Instituto de Pesquisas Energéticas e Nucleares (IPEN/CNEN), São Paulo, Brazil.

ABSTRACT: The high rates of antibiotics use in hospitals have resulted in a condition where multidrug-resistant pathogens have become a severe threat to the human health worldwide. Therefore, there is an increasing necessity to identify new antimicrobial agents that can inhibit the multidrug-resistant bacteria and biofilm formation. In this study, antibacterial and anti-biofilm activities of tryptophan silver nanoparticles (TrpAgNP) were investigated. The TrpAgNPs were synthesized by photoreduction method, and the influence of irradiation time and concentration of reagents were analyzed. The nanoparticles were characterized by transmission electron microscopy, Zeta Potential and (UV)-absorption spectra. The antibacterial activity of TrpAgNPs was tested for antibiotic-resistant and susceptible pathogens, *Staphylococcus aureus*, *Staphylococcus epidermidis*, *Escherichia coli*, *Citrobacter freundii*, *Klebsiella pneumoniae*, *Salmonella typhimurium*, and *Pseudomonas aeruginosa*, evaluating the influence of photoreduction parameters in bactericidal effect. The results have shown that TrpAgNPs solutions with lower tryptophan/silver nitrate (AgNO₃) ratio and higher AgNO₃ concentration have higher bactericidal action against bacteria with inhibition of ~100% in almost all studied bacterial strains. The antimicrobial activity of TrpAgNPs within biofilms generated under static conditions of antibiotic-resistant and susceptible strains of *S. aureus*, *S. epidermidis*, *E. coli*, *K. pneumoniae*, *C. freundii*, and *P. aeruginosa* was also investigated. The results showed that TrpAgNPs have an inhibitory effect against biofilm formation, exceeding 50% in the case of Gram-negative bacteria (*E. coli*, *K. pneumoniae*, *C. freundii*, and *P. aeruginosa*—54.8% to 98.8%). For Gram-positive species, an inhibition of biofilm formation of 68.7% to 72.2% was observed for *S. aureus* and 20.0% to 40.2% for *S. epidermidis*.

KEYWORDS: tryptophan, silver nanoparticles, photoreduction, antimicrobial activity, anti-biofilm

RECEIVED: December 20, 2018. **ACCEPTED:** January 20, 2019.

TYPE: Original Research

FUNDING: The authors are grateful to the FAPESP (2014/06960-9) and CNPq, Brazilian funding agencies, for their financial support.

DECLARATION OF CONFLICTING INTERESTS: The author(s) declared no potential conflicts of interest with respect to the research, authorship, and/or publication of this article.

CORRESPONDING AUTHOR: Lilia Coronato Courrol, Laboratório de Lasers e Óptica Biomédica Aplicada and Departamento de Física, Universidade Federal de São Paulo, Diadema SP 09972-270, Brazil.
Email: lccourrol@gmail.com

Introduction

The growing number of immunocompromised patients in the last decades has increased the incidence of bacterial infections. The excessive human use of antibiotics for prophylaxis or therapy has exerted selective pressure favoring the resistance of several pathogens, especially in nosocomial infections.¹

Microbial cells can adhere to each other on some living or non-living surfaces within a self-produced matrix of extracellular polysaccharides (EPSs), proteins, and DNA forming a so-called biofilm.² The National Institutes of Health (NIH) revealed that approximately 65% of all microbial infections and 80% of all long-term infections are associated with biofilms. Bacterial biofilm is less accessible to antibiotics and human immune system and thus cause a great warning to public health because of its participation in a variety of infectious diseases. This resistance has been attributed to the failure of antibiotics to penetrate biofilms and the induction of multidrug efflux pumps of biofilm-specific phenotypes.³

Stronger antibacterial and anti-biofilm activity synergistic or enhancement can be obtained when antibiotics are used in the presence of other compounds, such as nanocompounds. Various nanoparticles (NPs) are often reported as having inhibitory effect against biofilm cells.^{3–7} Silver nanoparticles (AgNPs) have powerful and natural antibiotic and antibacterial agents which exhibited antibacterial properties against some Gram-positive and Gram-negative bacteria.^{8,9} For this reason, there is an effort to incorporate AgNPs into a wide range of medical devices, food packages, and personal-care products. The antimicrobial potential of NP compounds may depend on their sizes, charges, and stability to control biofilm. Silver nanoparticles can bind cell membrane structures, destabilizing the membrane potential and causing proton leakage.^{10,11}

Different synthesis routes such as chemical, physical, or biological methods can be used for synthesizing AgNPs.^{12–16} The use of amino acids in AgNPs synthesis has been described in the literature as a simple, environmentally friendly, and cost-effective method.^{17–23} Tryptophan is an essential amino acid



Table 1. Reagents concentrations of TrpAgNPs and Xenon irradiation time.

FRACTION	TRYPTOPHAN (mmol/L)	AgNO ₃ (mmol/L)	Trp/AgNO ₃ RATIO	FRACTION	Xe IRRADIATION TIME (MINUTE)
TrpAg1	2.99 (±0.01)	0.18 (±0.01)	17:1	1'	5
				1''	10
				1'''	15
TrpAg2	3.04 (±0.01)	0.48 (±0.01)	6:1	2'	5
				2''	10
				2'''	15
TrpAg3	3.02 (20.01)	0.81 (±0.01)	4:1	3'	5
				3''	10
				3'''	15
TrpAg4	3.03 (±0.01)	1.41 (±0.01)	2:1	4'	5
				4''	10
				4'''	15

Abbreviations: Trp, tryptophan; AgNO₃, silver nitrate; Xe, Xenon.

with the ability to absorb and emit electromagnetic radiation in the ultraviolet (UV) range. Moreover, tryptophan has some advantages such as solubility in water, biocompatibility, and high reducing/stabilizing functionality.

Tomita et al²⁰ reported the bactericidal effect of TrpAgNPs produced by photoreduction in strains of *Escherichia coli*, *Pseudomonas aeruginosa*, *Staphylococcus epidermidis*, *Serratia marcescens*, and *Enterococcus faecalis*, using the microdilution test. The effect of TrpAgNPs synthesized by a femtosecond laser system proved high bactericidal efficiency against *E. coli*.²⁴ Dojčilović et al²⁵ showed an increase in the intensity of fluorescence toward the interior of the cells, indicating that *E. coli* internalized the tryptophan functionalized nanoparticles.

In this study, inhibitory and anti-biofilm activity of TrpAgNPs was investigated against reference bacteria and clinical isolates *Staphylococcus aureus*, *S. epidermidis*, *E. coli*, *Citrobacter freundii*, *Klebsiella pneumoniae*, *Salmonella typhimurium*, and *P. aeruginosa*, evaluating the influence of illumination time and concentration of the reagents used in the photoreduction process, on the bactericidal effect. The antimicrobial activity of TrpAgNPs within biofilms generated under static conditions of drug-resistant and susceptible strains *S. aureus*, *S. epidermidis*, *E. coli*, *K. pneumoniae*, *C. freundii* and *P. aeruginosa* was also investigated.

Materials and Methods

TrpAgNPs synthesis

Silver nanoparticles were synthesized mixing tryptophan (Vetec) with AgNO₃ (Sigma-Aldrich Brasil), with concentrations as described in the Table 1 followed by the addition of 100 mL of Milli-Q water. These solutions were stirred in vortex mixer for 5 minutes. Volumes of 10 mL of the prepared solutions were illuminated with a 300 W Xenon lamp (Cermac, Excelitas Technology) for 5, 10 and 15 minutes (x', x'' and x''', where x is the sample number as shown in the Table 1). The Xe lamp was positioned 10 cm away from the recipient containing

the solution, and the illuminated region covered exactly the recipient diameter, with a 3.6 W/cm² estimated intensity.

Characterization of TrpAgNPs

Spectrophotometry analyzes in the UV—visible (Vis) region were performed with the UV-Vis Shimadzu MultiSpec 1501 spectrophotometer. The measurements were carried out in a 10-mm optical path quartz cuvette in the range 250 to 800 nm.

The stability of the colloidal suspension was analyzed by Zeta potential measurements using the Zetasizer Nano ZS Malvern apparatus. Microscopic analyses were performed on a LEO 906E transmission electron microscope (Zeiss, Germany).

Method for in vitro evaluating antimicrobial activity

The micro-organisms used in this assay were as follows: *S. aureus* American Type Culture Collection (ATCC) 25923, *S. epidermidis* (clinical strain isolated from cutaneous abscesses), *E. coli* ATCC 25922, clinical strains of *E. coli* O44:H18 042 (EAEC),²⁶ *C. freundii* and *K. pneumoniae* isolated from diarrhea, *Salmonella thiphymurium* ATCC 14028, and *P. aeruginosa* ATCC 27853. The clinical strains present the following resistance profile: *S. epidermidis* (penicillin and streptomycin), *E. coli* O44:H18 042 (chloramphenicol, tetracycline, and streptomycin), *C. freundii* (sulfamethoxazole/trimethoprim, amoxicillin/clavulanic acid, and cephalothin), and *K. pneumoniae* (tetracycline and streptomycin).

The antimicrobial activity of the TrpAgNPs was tested in triplicate in 96-well plates, according to the guidelines of CLSI. Aliquots of 50 µL of Mueller-Hinton (MH) broth,²⁷ with bacterial inoculum adjusted to approximately 10⁶ CFU/mL, was applied in the microplates containing 50 µL of TrpAgNPs solutions (described in the Table 1) diluted in MH (20 µL of TrpAgNPs + 180 µL of MH). The final volume in each well

was 100 μL with 10^4 CFU/well and the final dilution of TrpAgNPs of 10 times. A positive growth control containing only culture medium and the strains under study was also prepared. The 100 μL of MH liquid culture medium was used as negative control in the study.

After inoculation, the plates were incubated at 37°C for 24 hours. After this time, the turbidity of the cultures was measured in an enzyme-linked immunosorbent assay (ELISA) reader (Multiskan® EX (Thermo Fisher Scientific, EUA) at 595 nm to assess bacterial growth. The results were expressed as inhibition percentage of optical density (OD) against a control (micro-organisms in the absence of test solutions). The percentage of cell inhibition was calculated by the following formula

$$\% \text{Cell inhibition} = \frac{\left[\text{Control at OD}_{595 \text{ nm}} - \text{Test at OD}_{595 \text{ nm}} \right]}{\text{Control at OD}_{595 \text{ nm}}} \times 100$$

The statistical test of antimicrobial activity assays is presented in the Figure 4 showing the averages of three measures obtained in cell inhibition calculation.

Biofilm inhibition assay

Biofilm production on polystyrene surface by bacterial strains after 24 hours of incubation was assayed following the method described by Sheikh et al (2001)²⁸ with slight modifications. Overnight bacterial cultures of *E. coli* ATCC 25922, *E. coli* O44:H18 042 (EAEC)²⁶, *K. pneumoniae*, *P. aeruginosa* ATCC 27853, *C. freundii*, *S. epidermidis* and *S. aureus* ATCC 25923 were grown in Tryptic soy broth (TSB) under static conditions and were inoculated into fresh Luria Bertani (LB) broth at a 1:1000 dilution in 96-well microplates in a final volume of 200 μL . This broth was supplemented with TrpAgNPs (Fractions 4', 4'', and 4''') with 3.03 mmol/L of tryptophan and 1.41 mmol/L of AgNO_3 and Xe irradiation by 5, 10 and 15 minutes, presenting a final dilution of 10 times. The wells with only medium served as blank, biofilm of micro-organisms served as control, and biofilm treated with TrpAgNPs served as test. These plates were incubated at 37°C for 24 hours. After the incubation period, the planktonic cells along with the media were discarded, and the preparation was washed with phosphate-buffered saline (PBS). Biofilm was fixed with 200 μL of 75% ethanol per well for 10 minutes, washed three times to remove the ethanol and stained with 0.5% crystal violet (CV) solution for 5 minutes. After PBS washings, the plates were air-dried, and the CV was solubilized by the addition of 200 μL of 95% ethanol per well. After 2 minutes at room temperature, 150 μL were transferred to a microtiter plate, and the absorbance was determined with an ELISA plate reader (Multiskan EX: Thermo Fisher Scientific, USA) at 595 nm. All assays were performed in triplicates. The biofilm inhibition by AgNPs was calculated using the formula.²⁸

$$\% \text{ Biofilm inhibition} = \frac{\left[\text{Control at OD}_{595 \text{ nm}} - \text{Test at OD}_{595 \text{ nm}} \right]}{\text{Control at OD}_{595 \text{ nm}}} \times 100$$

The statistical test of anti-biofilm assays is presented in the Figure 5 showing the averages of three measures obtained in biofilm inhibition calculation.

Results

To verify if the bactericidal effect of TrpAgNPs is dependent on the optical properties of the particles, synthesis of TrpAgNPs were carried out with different illumination times and concentration of the reagents.

TrpAgNPs characterization

The UV-Vis spectra from synthesized samples are shown in the Figure 1. As it can be seen in this figure, before Xe illumination, only tryptophan absorption band is observed in the spectra around 270 nm. After irradiation, the surface plasmon resonance (SPR) band can be observed around 450 nm. The increase in the AgNO_3 concentration cause a bathochromic shift of SPR band and increase in the spectral background. Figure 1 shows that the suspension named TrpAg 2 (molar ratio L-Trip: AgNO_3 6:1), exposed to the Xe lamp for 10 minutes, has the more symmetrical plasmonic band; indicating that these conditions resulted in a more homogeneous. Images of electron transmission microscopy (Figure 2B) and average size distribution (Figure 3) confirmed that in these conditions, spherical AgNPs are present with medium diameters of ~13.4 nm. Figures 2A, C and D show the images of TrpAg1, TrpAg3, and TrpAg4, respectively, prepared with exposure to the Xe lamp for 10 minutes. In these suspensions, the particles are more polydisperse and with more agglomerates. Tryptophan with Ag4 irradiated by 15 minutes presents an enlargement in the SPR band and multi-peaks fit evidence the presence of rods observed in the electron microscopy image (Figure 1D). The pH of the TrpAg solutions before irradiation ranged from 7.1 to 6.3 (TrpAg1 and TrpAg4, respectively) and after irradiation by 15 minutes from 7.4 to 4.3 (TrpAg1''' and TrpAg4''', respectively).

The TrpAg1 and TrpAg2 solutions have Zeta Potential >−30 mV, which means that the formed colloid system is highly stable. For TrpAg3 and TrpAg4, the potentials range from −25 to −28 mV, indicating moderately stable colloids.

Antimicrobial and anti-biofilm activities

Silver nanoparticles prepared with tryptophan were investigated for their bactericidal effect, and the results are shown in the Figure 4. In this figure, it is possible to observe that nanoparticles presented an accentuated antimicrobial activity especially for *S. epidermidis*. TrpAg4 irradiated for 5 minutes demonstrated inhibitory effect of 100% for all studied strains.

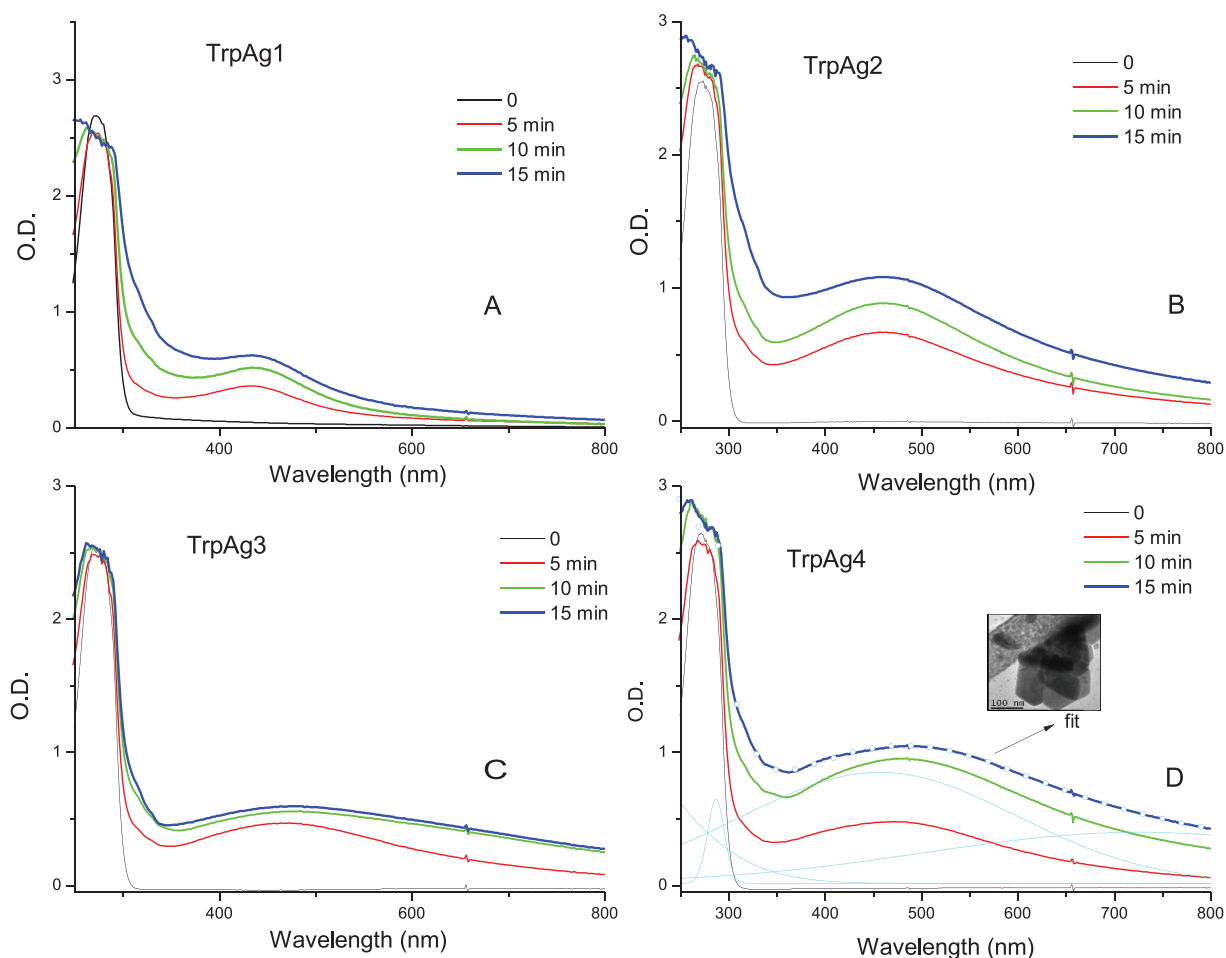


Figure 1. UV-Vis spectra of TrpAgNPs before and after different exposure times of the Xenon lamp (5, 10 and 15 minutes) for samples (A) TrpAg1, (B) TrpAg 2, (C) TrpAg 3, and (D) TrpAg 4.

Inset figure shows multi-peaks fit for SPR band and electron microscopy image for TrpAg4 irradiated by 15 minutes.

The fraction 4^{''} and 4^{'''} showed an elevated inhibitory effect over Gram-negative bacteria, *E. coli*, EAEC 042, *K. pneumoniae*, *S. Thiphymurium*, and *P. aeruginosa*, whereas the other fractions showed a lower or none effect against this group.

The results obtained for impact of TrpAg4 nanoparticles in the biofilm formation can be observed in the Figure 5. We observed an inhibitory effect against biofilm formation, exceeding ~90% in the case of Gram-negative bacteria *E. coli*, *P. aeruginosa*, *C. freundii*, and EAEC 042. For *K. pneumoniae*, the growth inhibition was in the range 54.9% and 88.0%. For Gram-positive species, an inhibition of biofilm formation of 67.2% to 71.8 % was observed for *S. aureus* and 20.0% to 40.2% for *S. epidermidis*.

Discussion

Photoreduction process is carried out to convert the AgNO_3 , in which the silver atoms have oxidation states of +1 (Ag^+), into the metallic silver. The reduction of the metallic ion occurs through the donation of electrons by the oxidized species. In this process, photons from the Xenon lamp are also responsible for the consumption/modification of tryptophan present in the solution. Some studies suggest that the

modification of tryptophan to form a Trp-Ag system passes through the oxidation of tryptophan.²³ Tryptophan also serves as a capping agent to prevent the nanoparticle agglomeration.

Silver nanoparticles have multiple mechanisms of antibacterial action.²⁹ Silver nanoparticles prepared with tryptophan can attach to the bacterial cell wall and infiltrate it, leading to membrane damage and cellular content leakage. Silver nanoparticles prepared with tryptophan or Ag^+ can bind to the protein present in the cell membrane, induce reactive oxygen species, lipid peroxidation, DNA damage, and reduce adenosine triphosphate (ATP) generation, which finally results in bacteria death.³⁰ Figure 4 indicates that TrpAg4 (Table 1) promoted the higher antimicrobial activity against all studied strains. In this case, silver concentration is the highest and seems to influence more in the antimicrobial activity than the particle shape and size distribution.

Gram-positive cell walls contain high peptidoglycan concentrations, whereas in the case of the Gram-negative cells, this peptidoglycan is restricted to a thin layer between the cytoplasmic membrane and the outer membrane. Peptidoglycan serves as a cell wall "sponge" attracting tryptophan in Gram-positive

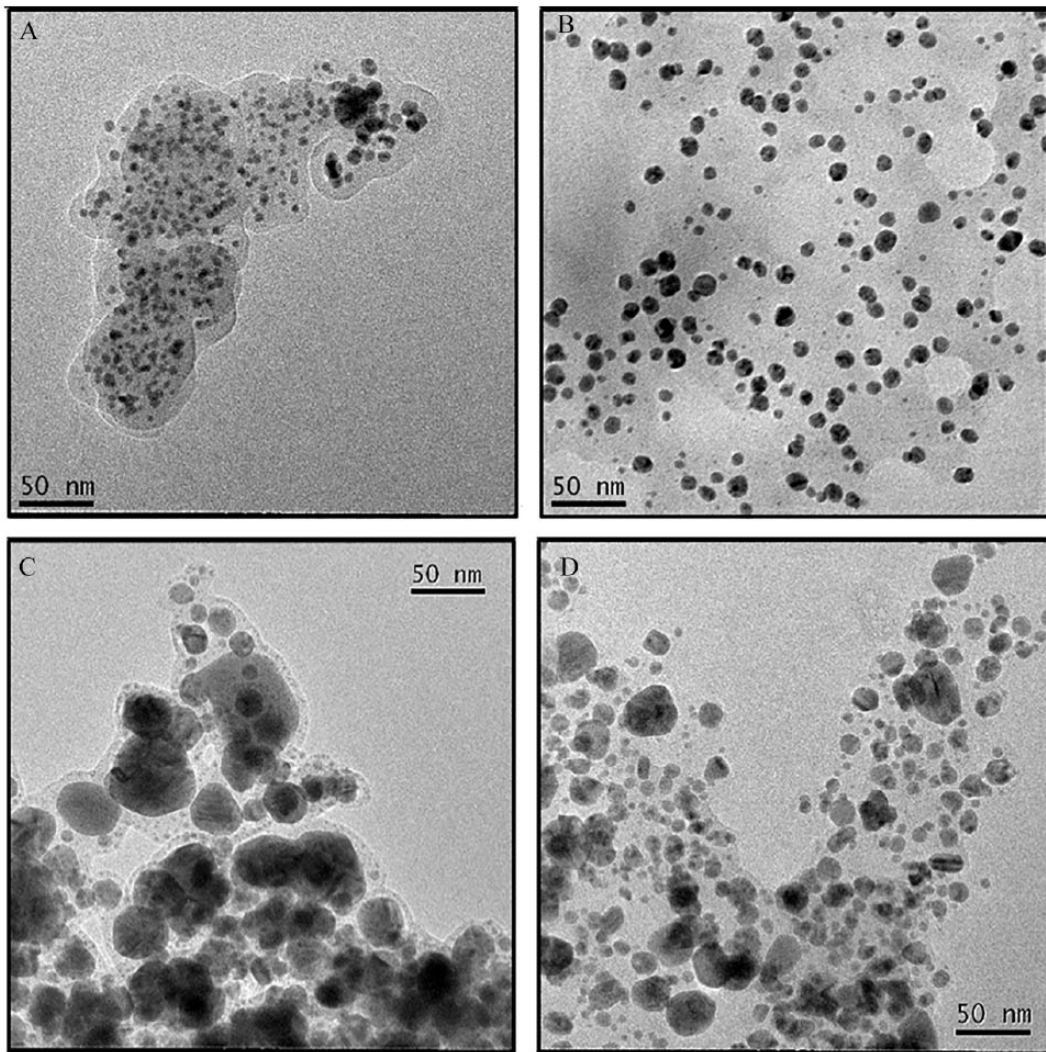


Figure 2. Transmission electron microscopy image of (A) TrpAg1, (B) TrpAg2, (C) TrpAg3 and (D) TrpAg4 (Xe 10 minutes).

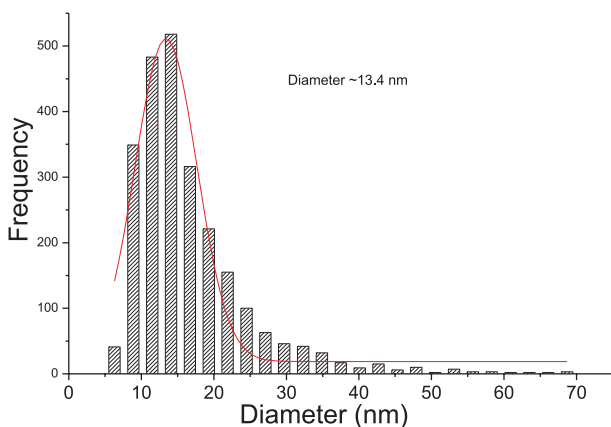


Figure 3. Size distribution histogram obtained for the sample TrpAg2 illuminated with Xenon lamp by 10 minutes.

bacteria. Therefore, the presence of high levels of peptidoglycan facilitates the attachment of TrpAgNPs, and probably for this reason, TrpAgNPs show more activity against Gram-positive bacteria.

Bacteria within a biofilm are several orders of magnitude more resistant to antibiotics, compared with planktonic bacteria. The structure of the extracellular polysaccharide (EPS) matrix of biofilms is composed of one or more of extracellular polysaccharides, DNA, and proteins. EPS matrix protects bacteria cells, in deeper layers, against antimicrobial agents possibly by limiting the diffusion of these agents.³¹ Biofilms are linked to various human diseases, for example, long-term lung, wound, and ear infections and can colonize on medical devices such as catheters and implants. The nanoparticles can easily infiltrate into the matrix which acts as a barrier for many antibiotics.⁴

The interactions between TrpAgNPs and the biofilm occur by transport of TrpAgNPs to the vicinity of the biofilm, attachment to the biofilm surface, and migration within the biofilm.²⁹ Silver nanoparticles prepared with tryptophan showed effective inhibition of biofilm formation of *E. coli* O44:H18 042(EAEC), a multidrug-resistant diarrheagenic *E. coli* responsible for persistent diarrhea, and *P. aeruginosa* that beyond its natural resistance to many drugs, has high ability to

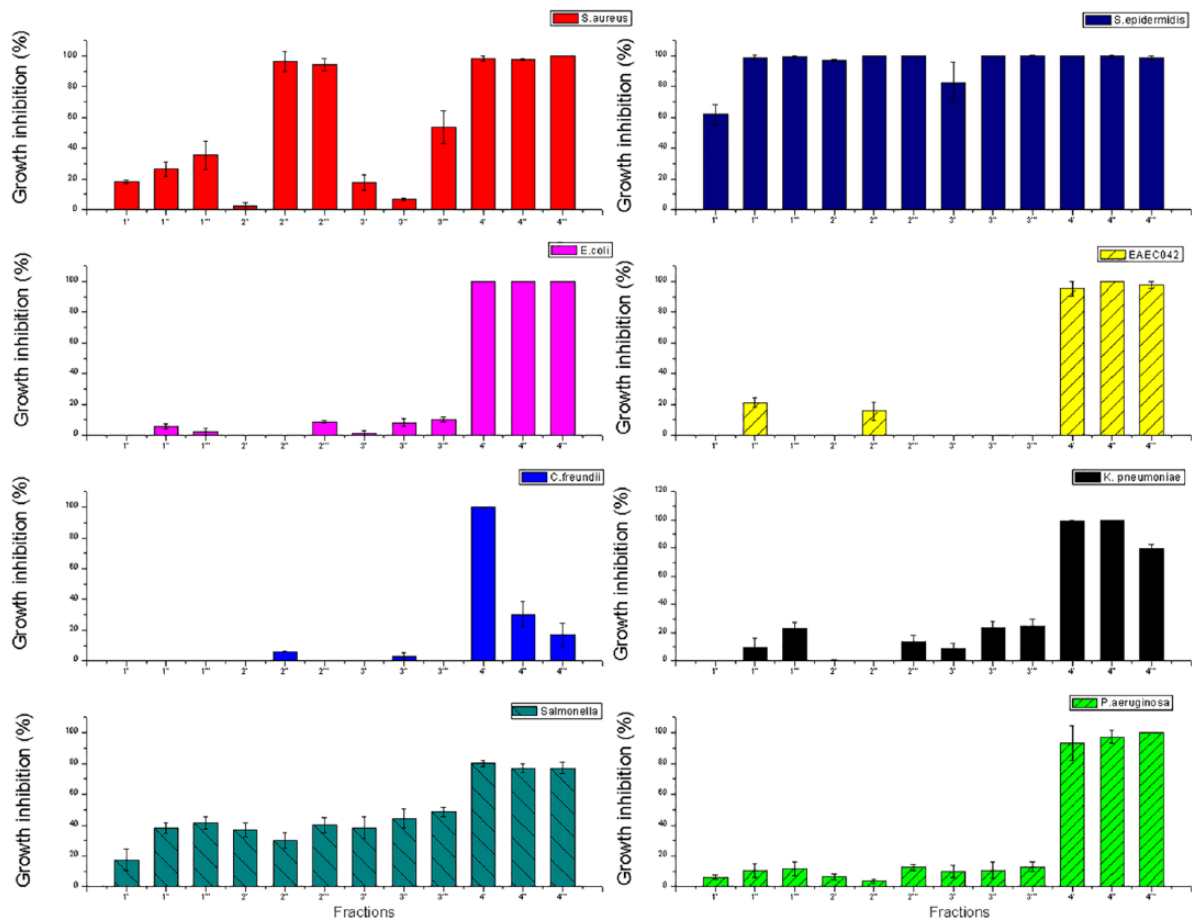


Figure 4. Antimicrobial activity of TrpAgNPs against *Staphylococcus aureus* ATCC 25923, *Staphylococcus epidermidis*, *Escherichia coli* ATCC 25922, *E. coli* O44:H18 O42 (EAEC), *Citrobacter freundii*, *Klebsiella pneumoniae*, *Salmonella Typhimurium* ATCC 14028, and *Pseudomonas aeruginosa* ATCC 27853 after 24 hours of incubation with different concentrations and irradiation times of TrpAgNPs indicated in the Table 1. The error bar denotes the standard error.

form biofilm. These results show that the nanoparticles, besides infiltrating the bacterial cell, are also able to overcome the mucus barrier that the biofilm forms indicating that the TrpAgNPs not only inhibited the growth but also the ability of the organism to synthesize EPS.

When the TrpAgNP approaches a surface, proteins and other biomolecules that reside long enough on the TrpAgNP will mediate subsequent interactions.²⁹ Silver nanoparticles prepared with tryptophan may directly diffuse through the glycocalyx matrix layer through the pores and may disclose antimicrobial function.⁶ They might be involved in neutralizing the adhesive substances, thus preventing biofilm formation. Another possible mechanism that contributes to TrpAgNP accumulation within the matrix is the active outgrowth of the biofilm, forming new layers above the surface-deposited NPs, and in this case, penetration of NPs into the biofilm matrix is not necessary.²⁹

Conclusions

In conclusion, this study describes the antibacterial and anti-biofilm efficacy of the AgNPs synthesized using tryptophan by photoreduction method.

Optical parameters of NPs synthesized have influence in antibacterial activity and the most effective formulation had Trp/AgNO₃ ratio ~2:1. For all tested synthesis conditions, TrpAgNPs showed elevated antimicrobial activity against *S. aureus* and *S. epidermidis*. Silver nanoparticles prepared with tryptophan exhibited effective inhibition of biofilm formation of *E. coli* O44:H18 O42(EAEC), a multidrug-resistant diarrheagenic *E. coli* responsible for persistent diarrhea and *P. aeruginosa* that, beyond its natural resistance to many drugs, has a high ability to form biofilm. Silver nanoparticles prepared with tryptophan were found to effectively prevent the formation and kill bacteria in established biofilm structures and may be useful for the prevention and treatment of biofilm-related infections.

Author Contributions

All authors reviewed and approved the final manuscript.

Disclosures and Ethics

As a requirement of publication, authors have provided to the publisher signed confirmation of compliance with legal and ethical obligations including but not limited to the following: authorship and contributor ship, conflicts of interest, privacy and confidentiality, and (where applicable) protection of human and animal research subjects.

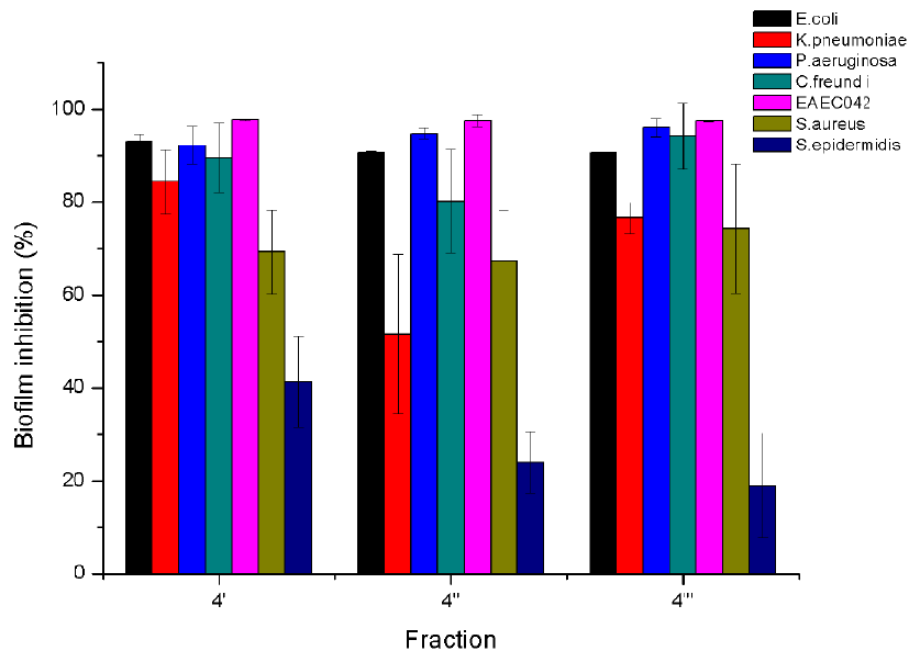


Figure 5. Average percentage inhibition of biofilm formation. Semi-quantitative biofilm inhibition assay was performed using TrpAgNPs against *Escherichia coli* ATCC25922, *Klebsiella pneumoniae*, *Pseudomonas aeruginosa* ATCC 27853, *Citrobacter freundii*, *Escherichia coli* O44:H18 042 (EAEC), *Staphylococcus aureus* ATCC 25923 and *S. epidermidis*. after 24 hours of incubation. The error bar denotes the standard error.

The authors have read and confirmed their agreement with the ICMJE authorship and conflict of interest criteria. The authors have also confirmed that this article is unique and not under consideration or published in any other publication and that they have permission from rights holders to reproduce any copyrighted material.

ORCID iDs

Carla Regina Borges Lopes  <https://orcid.org/0000-0002-6808-7152>

Camila Bueno Pacheco Pereira  <https://orcid.org/0000-0002-6007-5384>

Marcia Regina Franzolin  <https://orcid.org/0000-0003-0654-639X>

REFERENCES

- Zilberberg MD, Shorr AF, Micek ST, Vazquez-Guillamet C, Kollef MH. Multi-drug resistance, inappropriate initial antibiotic therapy and mortality in Gram-negative severe sepsis and septic shock: a retrospective cohort study. *Crit Care*. 2014;18:596. doi:10.1186/s13054-014-0596-8.
- Algburi A, Comito N, Kashtanov D, et al. Control of biofilm formation: antibiotics and beyond [published online ahead of print January 17, 2017]. *Appl Environ Microbiol*. doi:10.1128/aem.02508-16.
- Ramasamy M, Lee J. Recent nanotechnology approaches for prevention and treatment of biofilm-associated infections on medical devices. *Biomed Res Int*. 2016;2016:1851242. doi:10.1155/2016/1851242.
- Hemeg HA. Nanomaterials for alternative antibacterial therapy. *Int J Nanomed*. 2017;12:8211–8225. doi:10.2147/ijn.s132163.
- Qayyum S, Khan AU., Nanoparticles vs. biofilms: a battle against another paradigm of antibiotic resistance. *Med Chem Comm*. 2016;7:1479–1498. doi:10.1039/c6md00124f.
- Peulen T-O, Wilkinson KJ. Diffusion of nanoparticles in a biofilm. *Environ Sci Tech*. 2011;45:3367–3373. doi:10.1021/es103450g.
- Natan M, Banin E. From nano to micro: using nanotechnology to combat microorganisms and their multidrug resistance. *Fems Microbiol Rev*. 2017;41:302–322. doi:10.1093/femsre/fux003.
- Martinez-Gutierrez F, Boegli L, Agostinho A, et al. Anti-biofilm activity of silver nanoparticles against different microorganisms. *Biofouling*. 2013;29:651–660. doi:10.1080/08927014.2013.794225.
- Kalishwaralal K, BarathManiKanth S, Pandian SRK, et al. Silver nanoparticles impede the biofilm formation by *Pseudomonas aeruginosa* and *Staphylococcus epidermidis*. *Colloids Surfaces B*. 2010;79:340–344. doi:10.1016/j.colsurfb.2010.04.014.
- Gogoi SK, Gopinath P, Paul A, et al. Green fluorescent protein-expressing *Escherichia coli* as a model system for investigating the antimicrobial activities of silver nanoparticles. *Langmuir*. 2006;22:9322–9328. doi:10.1021/la060661v.
- Maillard J-Y, Hartemann P. Silver as an antimicrobial: facts and gaps in knowledge. *Crit Rev Microbiol*. 2013;39:373–383. doi:10.3109/1040841x.2012.713323.
- Zhang XF, Liu ZG, Shen W, et al. Silver nanoparticles: synthesis, characterization, properties, applications, and therapeutic approaches. *Int J Molec Sci*. 2016;17:34. doi:10.3390/ijms17091534.
- Pivetta RC, Auras BL, de Souza B, et al. Synthesis, photophysical properties and spectroelectrochemical characterization of 10-(4-methyl-bipyridyl)-5,15-(pentafluorophenyl) corrole. *J Photochem Photobiol A*. 2017;332:306–315. doi:10.1016/j.jphotochem.2016.09.008.
- Nath D, Banerjee P. Green nanotechnology—a new hope for medical biology. *Environ Toxicol Pharmacol*. 2013;36:997–1014. doi:10.1016/j.etap.2013.09.002.
- de Matos RA and Courrol LC. Saliva and light as templates for the green synthesis of silver nanoparticles. *Colloids and Surfaces a-Physicochemical and Engineering Aspects* 2014; 441: 539–543. DOI: 10.1016/j.colsurfa.2013.10.009
- Balaz M. Ball milling of eggshell waste as a green and sustainable approach: a review. *Adv Colloid Interf Sci*. 2018;256:256–275. doi:10.1016/j.cis.2018.04.001.
- Rawat KA, Kailasa SK. 4-Amino nicotinic acid mediated synthesis of gold nanoparticles for visual detection of arginine, histidine, methionine and tryptophan. *Sens Actuat B*. 2016;222:780–789.
- Shankar S, Rhim JW. Amino acid mediated synthesis of silver nanoparticles and preparation of antimicrobial agar/silver nanoparticles composite films. *Carbohydr Polym*. 2015;130:353–363. doi:10.1016/j.carbpol.2015.05.018.
- de Matos RA, Courrol LC. Biocompatible silver nanoparticles prepared with amino acids and a green method. *Amino Acids*. 2017;49:379–388. doi:10.1007/s00726-016-2371-4.
- Tomita RJ, de Matos RA, Vallim MA, et al. A simple and effective method to synthesize fluorescent nanoparticles using tryptophan and light and their lethal effect against bacteria. *J Photochem Photobiol B*. 2014;140:157–162. doi:10.1016/j.jphotobiol.2014.07.015.
- Shmarakov IO, Mukha IP, Karavan VV, et al. Tryptophan-assisted synthesis reduces bimetallic gold/silver nanoparticle cytotoxicity and improves biological activity. *Nanobiomed*. 2014;1:6. doi:10.5772/59684.
- Si S, Mandal TK. Tryptophan-based peptides to synthesize gold and silver nanoparticles: a mechanistic and kinetic study. *Chemistry*. 2007;13:3160–3168. doi:10.1002/chem.200601492.

23. Selvakannan P, Mandal S, Phadtare S, et al. Water-dispersible tryptophan-protected gold nanoparticles prepared by the spontaneous reduction of aqueous chloroaurate ions by the amino acid. *J Colloid Interf Sci.* 2004;269:97–102. doi:10.1016/s0021-9797(03)00616-7.
24. Courrol DD, Lopes CRB, Cordeiro TD, et al. Optical properties and antimicrobial effects of silver nanoparticles synthesized by femtosecond laser photo-reduction. *Optics Laser Tech.* 2018;103:233–238. doi:10.1016/j.optlastec.2018.01.044.
25. Dojčilović R, Pajovic JD, Bozanic DK, et al. A fluorescent nanoprobe for single bacterium tracking: functionalization of silver nanoparticles with tryptophan to probe the nanoparticle accumulation with single cell resolution. *Analyst.* 2016;141:1988–1996. doi:10.1039/c5an02358k.
26. Nataro JP, Baldini MM, Kaper JB, et al. Detection of an adherence factor of enteropathogenic escherichia-coli with a dna probe. *J Infect Dis* 1985; 152: 560–565. DOI: 10.1093/infdis/152.3.560.
27. CLSI. 2015. *Methods for dilution antimicrobial susceptibility tests for bacteria that grow aerobically; approved standard, 10th ed. CLSI document M07-A10.* Clinical and Laboratory Standards Institute, Wayne, PA.
28. Sheikh J, Hicks S, Dall'Agnol M, et al. Roles for Fis and YafK in biofilm formation by enteroaggregative Escherichia coli. *Mol Microbiol* 2001; 41: 983–997. DOI: 10.1046/j.1365-2958.2001.02512.x.
29. Ikuma K, Decho AW and Lau BLT. When nanoparticles meet biofilms—interactions guiding the environmental fate and accumulation of nanoparticles. *Front Microbiol* 2015; 6. DOI: 10.3389/fmicb.2015.00591.
30. Qayyum S, Oves M and Khan AU. Obliteration of bacterial growth and biofilm through ROS generation by facilely synthesized green silver nanoparticles. *Plos One* 2017; 12. DOI: 10.1371/journal.pone.0181363.
31. Kostakioti M, Hadjifrangiskou M and Hultgren SJ. Bacterial Biofilms: Development, Dispersal, and Therapeutic Strategies in the Dawn of the Postantibiotic Era. *Cold Spring Harb Perspect Med* 2013; 3. DOI: 10.1101/cshperspect.a010306.